Research Article | Vol. 28, No. 16 / 3 August 2020 / Optics Express 23105
Optics EXPRESS

Designing conformal cloaks by manipulating structures directly in the physical space

ZHANYI WANG,[1,2] YICHAO LIU,[1,3] TIANHANG CHENG,[2] FEI SUN,[1,4] AND SAILING HE[2,5]

[1] *Key Lab of Advanced Transducers and Intelligent Control System, Ministry of Education and Shanxi Province, College of Physics and Optoelectronics, Taiyuan University of Technology, Taiyuan 030024, China*
[2] *National Engineering Research Center for Optical Instruments, Centre for Optical and Electromagnetic Research, Zhejiang University, Hangzhou 310058, China*
[3] *liuyichao@tyut.edu.cn*
[4] *sunfei@tyut.edu.cn*
[5] *sailing@kth.se*

Abstract: The method to elaborately design the refractive index profile in the lower Riemann sheet of Zhukovski transformation plays an important role in the performance of this kind of conformal cloaks. However, for most proposed schemes, the mathematical calculations are complex. Here, we propose a more convenient method to design conformal cloaks by manipulating structures directly in the physical space. The designed cloak only needs symmetrical metal boundaries filled with normal dielectrics (refractive index ranges from 1 to 2) in the 'circular branch cut', which would be more feasible for future experimental implementation. Numerical simulations are performed by using the finite element method to validate our theoretical analysis.

1. Introduction

Transformation optics (TO) is a powerful tool to design extraordinary optical devices [1,2] by controlling electromagnetic fields. One of the most remarkable applications is the invisibility cloak. After the key paper by Pendry *et al*. [3] and the followed experiment by Schurig et al. [4], many different proposals have been given to design cloaks [5–13]. However, realization of these cloaks usually requires metamaterials with anisotropic and inhomogeneous parameters [9–13], which brings challenges to the experiments. Recently, Zheng *et al*. has experimentally demonstrated an omnidirectional cloak with some extreme-parameter [14], which is an improvement for the realization of full-parameter omnidirectional cloaks. Optical conformal mapping (OCM) [15–18] may simplify the complex material parameters by using isotropic dielectrics for two-dimensional cloaks [19–28]. However, the broad range and rapid change of the refractive index distribution make it still difficult to realize in practice [23–25]. In our previous work [27], optical-null-medium (ONM) [8,29,30] is used in the design of conformal cloaks to eliminate the geometrical dispersion and reduce the large index profile, where an effective optical design is constructed in the reference space and is then mapped to the physical space to obtain the material parameters. However, the boundaries of subwavelength channels and the concealed region designed in our previous design are asymmetric irregular curves, which is not easy to be fabricated. Actually, all previous designs on OCM cloaks are playing tricks in the lower Riemann sheet in the reference space [19–28], which inevitably involves complex calculations of the material parameters and unpredictable boundary shapes. In the present study, based on the perfect endoscope effect of ONM, we introduce the idea of "linking equivalent surfaces on the branch cut by ONMs in the physical space" and propose the method "manipulating structures directly in the physical space of Zhukovski transformation", which avoids the complex calculations during the designs and obtain OCM cloaks of arbitrary predesigned boundary shapes. Moreover, our

#395358 https://doi.org/10.1364/OE.395358
Journal © 2020 Received 17 Apr 2020; revised 23 Jun 2020; accepted 13 Jul 2020; published 20 Jul 2020

two-dimensional cloaks are omnidirectional and only ordinary materials (isotropic materials with $n < 2$ and metal boundaries) are used, which is more feasible for implementation.

2. Theoretical method

In this section, we demonstrate the principle of how to design an omnidirectional conformal cloak by manipulating structures directly in the physical space. Firstly, the concept of the Zhukovski transformation [15] is briefly introduced, which is a type of conformal mapping with the formula given by:

$$w = z + \frac{a^2}{z} \quad \text{or} \quad z = \frac{1}{2}\left(w \pm \sqrt{w^2 - 4a^2}\right) \tag{1}$$

where $z = x + iy$ and $w = u + iv$ denote complex coordinates in the physical space and the reference space, respectively. The reference space is composed of two Riemann sheets, which are connected by a line segment (branch cut) with length $4a$. The Zhukovski transformation maps the branch cut in the reference space to a circle with radius a in the physical space, which we call the 'circular branch cut' for convenience to emphasize it is mapped from the branch cut in the reference space although it is not really a branch cut in the physical space. The upper and lower Riemann sheets in the reference space are mapped to the exterior and interior of the 'circular branch cut' in the physical space, respectively. The refractive index distribution between the reference space and the physical space of Zhukovski transformation is given by [15]:

$$n = n_w \left|1 - \frac{a^2}{z^2}\right| \tag{2}$$

where n and n_w is the refractive index in the physical space and the reference space, respectively. In our design, only the refractive index distribution outside of the 'circular branch cut' in the physical space is calculated according to Eq. (2), which varies from 0 to 2. Materials inside the 'circular branch cut' are designed directly in the physical space.

In the previously reported conformal cloak designs with Zhukovski transformation [27,31–33], rays touching the branch cut in the upper Riemann sheet will enter into the lower Riemann sheet. Then, well-designed materials or structures (Eaton lens, Maxwell fisheye lens, metal walls, etc.) are used to guide them back to the upper Riemann sheet. Equation (1) and Eq. (2) are used to obtain the transformed curve boundaries and the refractive index distributions inside the 'circular branch cut' in the physical space.

Actually, for a perfect cloaking effect, the upper and lower semicircles of the 'circular branch cut' should be equivalent surfaces (equivalent curves in x-y plane for two dimensional cases) for the OCM cloaking design by Zhukovski transformation [15]. Therefore, the goal of the conventional OCM cloaking design is to link these two equivalent surfaces in the reference space, which is usually fulfilled by using complex optical lens, e.g., Maxwell fisheye lens in the lower Riemann sheet. The key idea of this study is linking the above equivalence surfaces by ONMs (i.e., subwavelength channels) directly in the physical space instead of the conventional lens with complex refractive index distributions in the reference space. Ideal ONM can be obtained by stretching a surface to a volume from the perspective of TO, which creates infinite equivalent surfaces along its main axis. Ideal ONM can project electromagnetic fields on one surface identically onto the other surface along its main axis [8,30], which performs as a perfect lens. In this study, simple metallic subwavelength channels with normal dielectrics (refractive index ranges from 1 to 2) are designed to realize the reduced ONMs, which perform as tunneling channels to link the two equivalent surfaces directly in the physical space.

The basic setup in the physical space for the designed OCM cloak is shown in Fig. 1, where three rays with different incident directions are plotted. The horizontal ray (colored purple) does not touch the 'circular branch cut' (white circle) and bypasses it. The other two rays touch the

Optics EXPRESS

branch cut, and then enter into the region inside the branch cut, which is filled with symmetrical subwavelength channels (colored green). The boundaries of subwavelength channels are marked in black. The red ray (with an incidence angle of 45°) and the blue perpendicular ray propagate straight in the subwavelength channels, cross the branch cut and then restore its original direction with the help of the OCM shell (colored yellow). The gray hexagonal region is the cloaking region. Note the rays can exit the 'circular branch cut' with an "correct" angle, which can be explained from the perspective of "phase preserving feature of two surfaces linked by ONMs". Two surfaces linked by the ONM perform as the equivalent surface: the electric field distribution (phase and amplitude) on one surface will be identically projected onto the other surface along the main axis of the ONM [8,30], which performs as a perfect lens. The ONMs can preserve the phase between two surface it links, which also ensures the phase gradient along the two surfaces are the same. The phase gradient along the surface (i.e., the wavevector parallel to the surface $k_{//}$) determines the angle between the propagation direction of the beam and the surface. Therefore, the rays can exit the second surface with a correct direction, i.e., the ray has the same angle between the second surface and the first surface. The subwavelength channels used to realize ONMs should be small enough (i.e., on the subwavelength order) to distinguish and preserve the phase gradient.

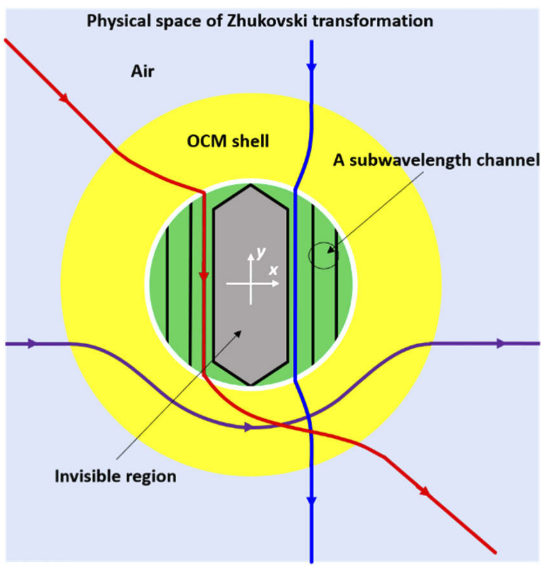

Fig. 1. Design diagram of the cloak in the physical space. Red, blue and purple lines indicate three ray trajectories with different incident directions. The region colored gray is the cloaking region. The green region can be filled with ZIMs or well-designed dielectrics. The black line segments indicate metal boundaries of subwavelength channels.

3. Design examples and numerical simulations

Three different structures of subwavelength channels are given to illustrate the cloak design using the above method. In the first example [Fig. 2(a)], the boundaries of the subwavelength channels are composed of polyline segments. For the other two designs, the boundaries of the subwavelength channels are part of an ellipse [Figs. 2(b) and 2(c)], and the difference between them is the location of the invisibility regions. In the following, numerical simulations are used to check the performance of the invisibility cloaks.

Optics EXPRESS

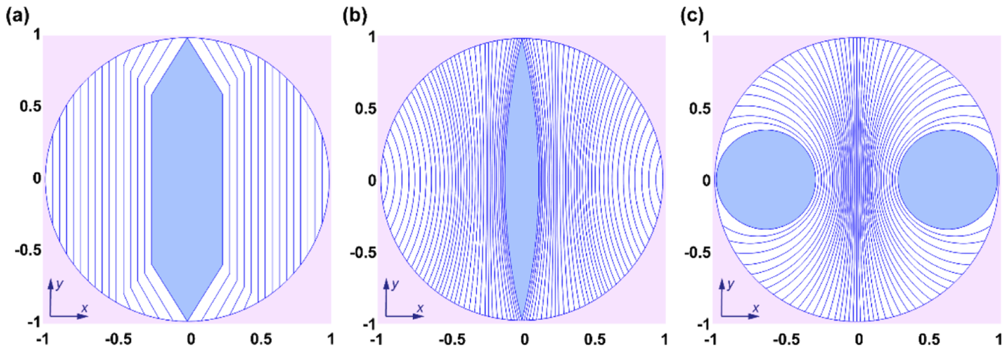

Fig. 2. Geometrical structures of three symmetrical cloaks designed by our method. (a) polyline channels; (b) elliptical channels with the central region concealed; (c) elliptical channels with the two concealed regions symmetrically distributed on the left and right sides. The regions in blue color are the cloaking regions.

We set a=1 m and truncate the cloak to a circle with a radius of 8 m. The cloak is surrounded by a perfect matched layer (PML) with a thickness of 2m. A background plane wave with TM polarization is set as the source. The materials outside the branch cut are magnetic materials, with $\varepsilon_r = 1$ and $\mu_r = n^2$. Structures inside the branch cut is subwavelength channels made up of impedance matched ZIMs ($\varepsilon_r = \mu_r = 0.01$) and perfect electric conductors (PEC) boundaries. To check the omnidirectional property of our cloaks, plane waves ($\lambda = 1.5a$) with three different incident angles (0°, 45°, 90°) impinge on the PEC object (colored white) with [Figs. 3(a)–3(c)] and without [Figs. 3(d)–3(f)] the cloaks, respectively. We use the second structure [Fig. 2(b)] in this example. Actually, any objects with arbitrary material parameters enclosed with the PEC boundary can be concealed. The distributions of the electric field patterns show that nearly no scattering appears with these three incident angles using our cloaks, while obvious scatterings occur without the cloaks.

The same good cloaking effects are found for the other two structures. The performance of the cloaks with the other two structures under incident plane waves ($\lambda = a$, and incident angle of 45°) is shown in Figs. 4(a)–4(b). Objects in the region colored white can be concealed.

The cloaks can be designed under different working frequencies as long as they satisfy the material parameters described above. Here, three different wavelengths (a, 2.125a, and 5a) are chosen for the incident plane wave (with an incident angle of 45°). The distributions of the electric field for the cloaks are shown in Figs. 5(a)–5(c). The zoom-in plots are shown in Figs. 5(d)–5(f).

Now we show a practical realization of the above cloak without ZIMs. The realization of the cloaks can be divided into two regions: the exterior and interior of the ‘circular branch cut’. Outside the ‘circular branch cut’, the regions of our cloaks are isotropic materials, with a refractive index from 0 to 2, which we have realized experimentally [22]. In the above simulations, metallic subwavelength channels filled with ZIMs are used to mimic the ONM. However, in experimental demonstration, the most difficult part of the realization of our cloaks is ZIMs, which usually require metamaterials with loss and limited bandwidth. Normal dielectrics can be used to simplify the cloaks without the ZIMs. In the present design, to obtain the cloaking effect, the index of each subwavelength channel should be chosen properly to make sure the phase delay in each subwavelength channel is an integer multiple of 2π at a certain frequency:

$$n_i = \frac{m\lambda}{L_i} \tag{3}$$

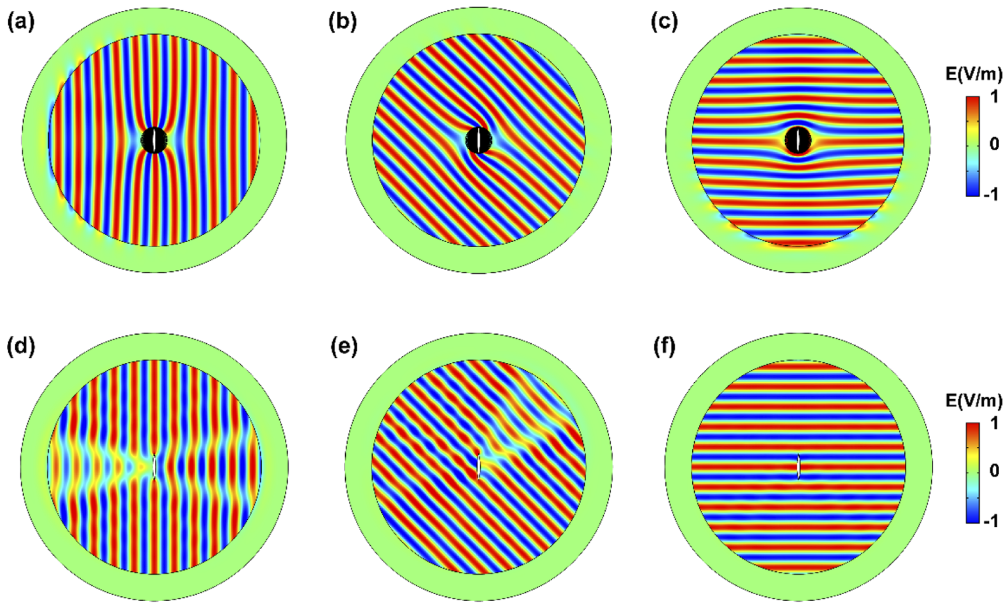

Fig. 3. Distributions of the electric field (for TM) for the PEC objects (a)-(c) with the cloak [shown in Fig. 2(b)] and (d)-(f) without the cloak. Three incident angles are (a), (d): 0°, (b), (e): 45°, and (c), (f): 90°. The regions in white color are the cloaking regions with PEC boundaries.

where n_i and L_i is the refractive index and length of the i-th subwavelength channel, respectively. λ is the wavelength in vacuum. The positive integer number m is carefully chosen to make sure that the value of n_i is between 1 and 2. Here, the designed working frequency is 0.3GHz and the designed refractive index value for each subwavelength channel is shown in Fig. 6(a), which ranges from one to two. Figure 6(b) shows the relative length L_i/λ, the refractive index n_i and the integer multiple number m of each subwavelength channel (only shows half of the subwavelength channels due to symmetry). For the first two subwavelength channels, m is not an integer number, and this is because we choose a relatively low value of the refractive index ($n_1 = 1$, $n_2 = 2$) to avoid local resonance and get a better performance. Our simplified cloak still has a good cloaking effect in the working frequency [Fig. 6(c) and (d)]. Materials in the interior of branch cut are greatly simplified to isotropic dielectrics (index between 1 and 2) and is homogenous in each subwavelength channel. The width of the subwavelength channels should be on the subwavelength order, which can be treated as the effective medium for the EM waves. From the perspective of effective medium theory, there is no lower bound on the width of the subwavelength channel. However, for the practical implementation, the width of the subwavelength channels cannot be too small (it should be wide enough for drilling holes on dielectric slabs). For fabrication, we can drill holes with different size or density on a dielectric disk and then split it into several parts, which represent dielectrics of each subwavelength channel [18]. Metal tapes can be used between each adjacent dielectric slab to form the boundary of each subwavelength channel. Although 70 subwavelength channels are used in Fig. 6(c) and (d), smaller number of subwavelength channels can still get a similar performance as shown in Fig. 6(e) and (f), where 30 subwavelength channels are used instead of 70.

Conventional conformal cloak with different profiles (i.e., with Eaton lens, Maxwell fisheye, or pure metal boundaries [23–25]) all have a large and rapid change of the refractive index inside the 'circular branch cut'. In the present work, although the refractive index inside the 'circular branch cut' is inhomogeneous, it is homogeneous inside each subwavelength channel. In addition,

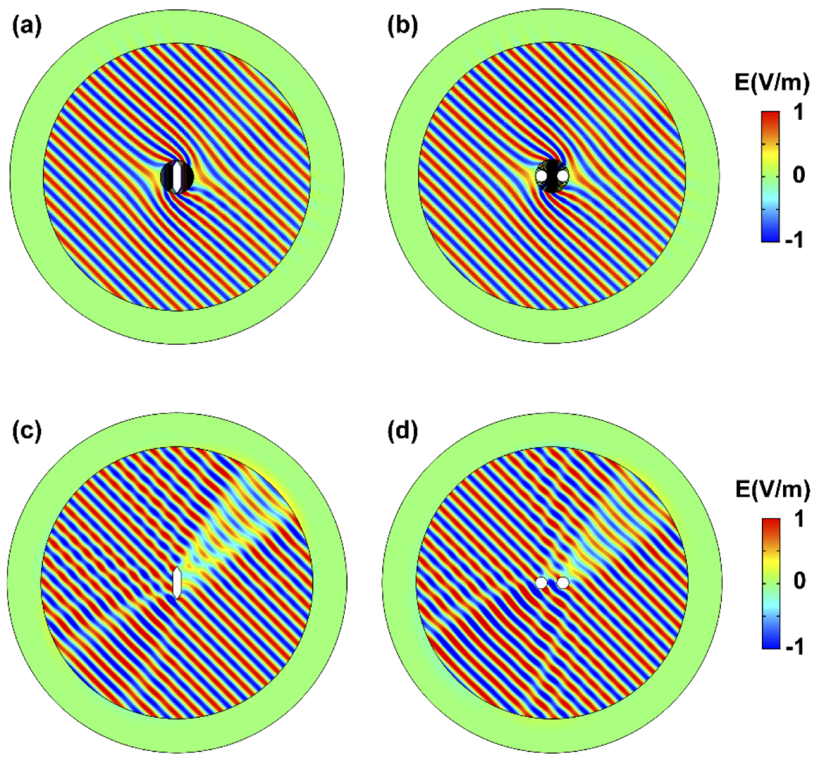

Fig. 4. Distributions of the electric field (for TM) for PEC objects (a)-(b) with the other two cloaks [shown in Figs. 2(a) and 2(c)] and (c)-(d) without the cloaks with an incident angle of 45°. The regions in white color are the cloaking regions with PEC boundaries.

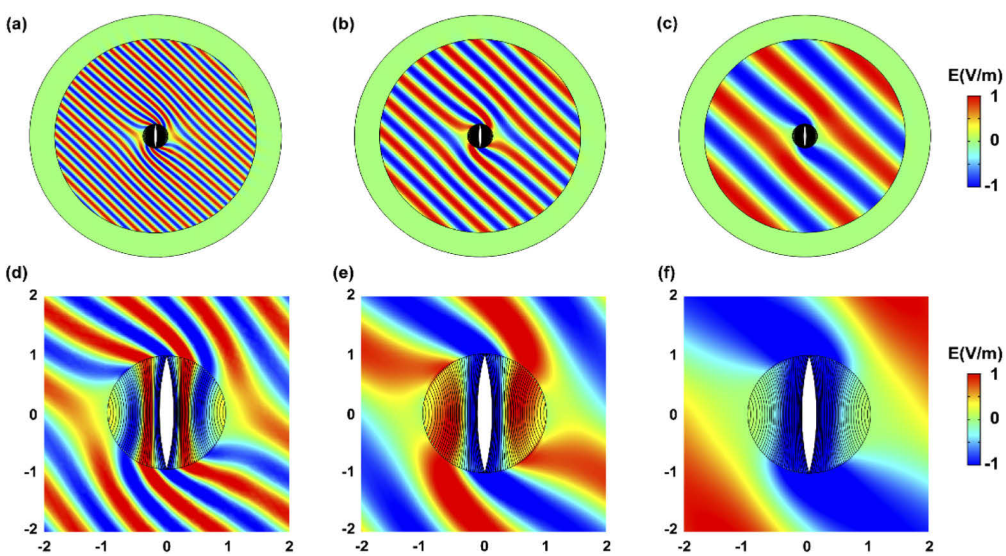

Fig. 5. Distributions of the x and y components of the electric field (for TM) for the second cloak (shown in Fig. 2(b)) under three different wavelengths of (a) a, (b) $2.125a$ and (c) $5a$. (d)-(f) are magnified plots of those in (a)-(c). The regions in white color are the cloaking regions with PEC boundaries.

Optics EXPRESS

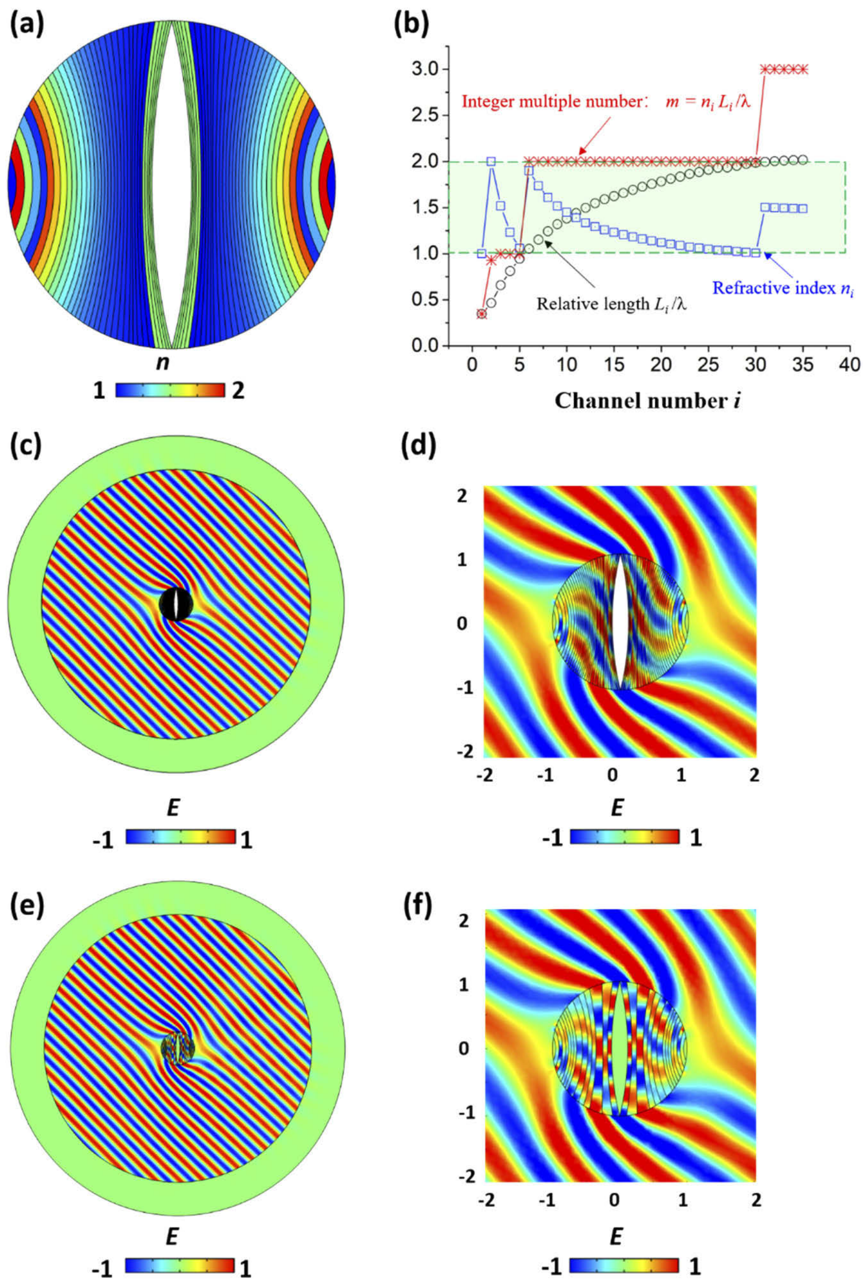

Fig. 6. (a) Refractive index distribution inside the branch cut of the simplified cloak (homogenous in each subwavelength channel). (b) Relative length L_i/λ, the refractive index n_i and the integer multiple number m of each subwavelength channel (only shows half of the subwavelength channels due to symmetry); the green region indicates the refractive index ranges from 1 to 2. (c)-(f) The distribution of the electric field (for TM waves at 0.3 GHz) for the PEC object covered by the simplified cloak (c) with 70 subwavelength channels and (e) with 30 subwavelength channels. (d) and (f) are the relative zoom-in plots.

the refractive index inside the 'circular branch cut' can be designed to a value between 1 and 2, i.e., the large and rapid change of the refractive index of the conventional conformal cloak is replaced by a relative flat and small value, which is a big improvement from the conventional one. Therefore, the proposed method "manipulating structures directly in the physical space" may play a role in promoting more feasible invisibility technology.

4. Summary

Considering all previous methods on OCM cloaks are making designs in the lower Riemann sheet in the reference space, and are then transformed back to the physical space [19–28], the traditional designing process inevitably leads to unpredictable materials (often needs a large and rapid change of the refractive index) and boundaries (e.g., asymmetric irregular curves) in the physical space. In this study, we propose the method "manipulating structures directly in the physical space" to design two-dimensional omnidirectional cloaks with symmetrical subwavelength channels with simple geometrical shapes and normal dielectrics (refractive index is between 1 and 2).

In conclusion, the novelty of the present work can be summarized as: Firstly, we abandon the conventional OCM cloak design process (i.e., design an optical loop in the lower Riemann sheet in the reference space and then transform it to the physical space) by manipulating symmetrical structures directly in the physical space. This idea provides us with more flexibility and less complexity in the conformal cloak design (e.g., there is no complex mathematical calculations during the design process). Secondly, the cloaking device designed by the proposed method has simpler structure with more flexibility than the previous one, i.e., arbitrary predesigned metal boundaries for both subwavelength channels and the concealed region, which provides convenience for real fabrication. As an example, omnidirectional OCM cloaks of simple geometrical shapes (polyline or elliptical channels) and realizable isotropic materials (refractive index is smaller than 2 in the whole device) are designed by the proposed method, which show very good scattering-suppression effect in numerical simulations.

Funding

National Key Research and Development Program of China (2017YFA0205700); National Natural Science Foundation of China (61905208, 61971300); Scientific and Technological Innovation Programs (STIP) of Higher Education Institutions in Shanxi (2019L0146, 2019L0159).

Disclosures

The authors declare no conflicts of interest.

References

1. H. Chen, C. T. Chan, and P. Sheng, "Transformation optics and metamaterials," Nat. Mater. **9**(5), 387–396 (2010).
2. M. Schmiele, V. S. Varma, C. Rockstuhl, and F. Lederer, "Designing optical elements from isotropic materials by using transformation optics," Phys. Rev. A **81**(3), 033837 (2010).
3. J. B. Pendry, D. Schurig, and D. R. Smith, "Controlling electromagnetic fields," Science **312**(5781), 1780–1782 (2006).
4. D. Schurig, J. J. Mock, B. J. Justice, S. A. Cummer, J. B. Pendry, A. F. Starr, and D. R. Smith, "Metamaterial electromagnetic cloak at microwave frequencies," Science **314**(5801), 977–980 (2006).
5. T. Ergin, N. Stenger, P. Brenner, J. B. Pendry, and M. Wegener, "Three-Dimensional Invisibility Cloak at Optical Wavelengths," Science **328**(5976), 337–339 (2010).
6. L. Xu and H. Chen, "Transformation optics with artificial Riemann sheets," New J. Phys. **15**(11), 113013 (2013).
7. M. M. Sadeghi, S. Li, L. Xu, B. Hou, and H. Chen, "Transformation optics with Fabry-Perot resonances," Sci. Rep. **5**(1), 8680 (2015).
8. F. Sun, B. Zheng, H. Chen, W. Jiang, S. Guo, Y. Liu, Y. Ma, and S. He, "Transformation Optics: From Classic Theory and Applications to its New Branches," Laser Photonics Rev. **11**(6), 1700034 (2017).

Optics EXPRESS

9. M. Bayati and M. Omoomi, “Analysis and design of an invisibility cloak based on transformation optics at microwave frequencies,” Turk. J. Electr. Eng. Comput. Sci. **25**(6), 4486–4495 (2017).
10. N. Landy and D. R. Smith, “A full-parameter unidirectional metamaterial cloak for microwaves,” Nat. Mater. **12**(1), 25–28 (2013).
11. H. Chu, Q. Li, B. Liu, J. Luo, S. Sun, Z. H. Hang, L. Zhou, and Y. Lai, “A hybrid invisibility cloak based on integration of transparent metasurfaces and zero-index materials,” Light: Sci. Appl. **7**(1), 50 (2018).
12. E. Moghbeli, H. R. Askari, and M. R. Forouzeshfard, “The effect of geometric parameters of a single-gap SRR metamaterial on its electromagnetic properties as a unit cell of interior invisibility cloak in the microwave regime,” Opt. Laser Technol. **108**, 626–633 (2018).
13. C. Y. Tay, M. Teniou, H. Roussel, and Z. N. Chen, “A non-singular transformation optics invisibility cloak by combining with scattering cancellation,” Phys. Scr. **94**(4), 045503 (2019).
14. B. Zheng, Y. Yang, Z. Shao, Q. Yan, N.-H. Shen, L. Shen, H. Wang, E. Li, C. M. Soukoulis, and H. Chen, “Experimental Realization of an Extreme-Parameter Omnidirectional Cloak,” Research **2019**, 1–8 (2019).
15. U. Leonhardt, “Optical conformal mapping,” Science **312**(5781), 1777–1780 (2006).
16. J. Zhang, J. B. Pendry, and Y. Luo, “Transformation optics from macroscopic to nanoscale regimes: a review,” Adv. Photonics **1**(01), 1 (2019).
17. J. B. Pendry, P. A. Huidobro, Y. Luo, and E. Galiffi, “Compacted dimensions and singular plasmonic surfaces,” Science **358**(6365), 915–917 (2017).
18. Y. Huang, Y. Zhang, J. Zhang, D. Liu, and Y. Luo, “A conformal transformation approach to wide-angle illusion device and absorber,” Nanophotonics. (2020).
19. J. P. Turpin, A. T. Massoud, Z. H. Jiang, P. L. Werner, and D. H. Werner, “Conformal mappings to achieve simple material parameters for transformation optics devices,” Opt. Express **18**(1), 244–252 (2010).
20. H. Y. Chen, U. Leonhardt, and T. Tyc, “Conformal cloak for waves,” Phys. Rev. A **83**(5), 055801 (2011).
21. Q. N. Wu, Y. D. Xu, H. Li, and H. Y. Chen, “Cloaking and imaging at the same time,” EPL **101**(3), 34004 (2013).
22. Y. Ma, Y. Liu, L. Lan, T. Wu, W. Jiang, C. K. Ong, and S. He, “First experimental demonstration of an isotropic electromagnetic cloak with strict conformal mapping,” Sci. Rep. **3**(1), 2128 (2013).
23. L. Xu and H. Y. Chen, “Logarithm conformal mapping brings the cloaking effect,” Sci. Rep. **4**(1), 6862 (2015).
24. L. Xu, H. Chen, T. Tyc, Y. Xie, and S. A. Cummer, “Perfect conformal invisible device with feasible refractive indexes,” Phys. Rev. B **93**(4), 041406 (2016).
25. H. Kan, L. Xu, Y. Xu, and H. Chen, “Conformal cloaks from a function composition,” EPL **117**(3), 34002 (2017).
26. L. Xu, T. Tyc, and H. Chen, “Conformal optical devices based on geodesic lenses,” Opt. Express **27**(20), 28722–28733 (2019).
27. Y. Liu, F. Sun, and S. He, “Omnidirectional Conformal Cloak Without Geometrical Dispersion,” Phys. Rev. Appl. **12**(6), 064009 (2019).
28. L. Xu and H. Y. Chen, “Conformal transformation optics,” Nat. Photonics **9**(1), 15–23 (2015).
29. F. Sun and S. He, “Optic-null space medium for cover-up cloaking without any negative refraction index materials,” Sci. Rep. **6**(1), 29280 (2016).
30. F. Sun and S. He, “Optical Surface Transformation: Changing the optical surface by homogeneous optic-null medium at will,” Sci. Rep. **5**(1), 16032 (2015).
31. T. Xu, Y. C. Liu, Y. Zhang, C. K. Ong, and Y. G. Ma, “Perfect invisibility cloaking by isotropic media,” Phys. Rev. A **86**(4), 043827 (2012).
32. Y. Liu, M. Mukhtar, Y. Ma, and C. K. Ong, “Transmutation of planar media singularities in a conformal cloak,” J. Opt. Soc. Am. **30**(11), 2280–2285 (2013).
33. Y. Liu, F. Sun, and S. He, “Controlling lightwave in Riemann space by merging geometrical optics with transformation optics,” Sci. Rep. **8**(1), 514 (2018).